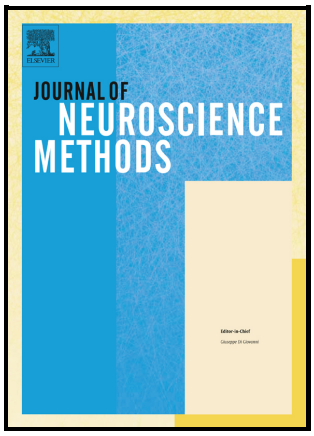

Differences in Conduction Velocities of Nerve Fibers Excited by Infrared and Electrical Stimulation

Louis VANDE PERRE, Javier CHÁVEZ CERDA, Soizic GOCHARD, Maxime VERSTRAETEN, Romain RAFFOUL, Catherine LEONARD, Jean DELBEKE, Riëm EL TAHRY, Simon-Pierre GORZA, Antoine NONCLERCQ

PII: S0165-0270(25)00068-8

DOI: https://doi.org/10.1016/j.jneumeth.2025.110427

Reference: NSM110427

To appear in: *Journal of Neuroscience Methods*

Received date: 19 November 2024
Revised date: 11 March 2025
Accepted date: 12 March 2025

Please cite this article as: Louis VANDE PERRE, Javier CHÁVEZ CERDA, Soizic GOCHARD, Maxime VERSTRAETEN, Romain RAFFOUL, Catherine LEONARD, Jean DELBEKE, Riëm EL TAHRY, Simon-Pierre GORZA and Antoine NONCLERCQ, Differences in Conduction Velocities of Nerve Fibers Excited by Infrared and Electrical Stimulation, *Journal of Neuroscience Methods,* (2025) doi:https://doi.org/10.1016/j.jneumeth.2025.110427

Differences in Conduction Velocities of Nerve Fibers Excited by Infrared and Electrical Stimulation

Louis VANDE PERRE*[1,2], Javier CHÁVEZ CERDA[1], Soizic GOCHARD[3], Maxime VERSTRAETEN[1], Romain RAFFOUL[1], Catherine LEONARD[4], Jean DELBEKE[5], Riëm EL TAHRY[5], Simon-Pierre GORZA[2], and Antoine NONCLERCQ[1]

[1] Bio-, Electro- and Mechanical- Systems (BEAMS), Université libre de Bruxelles, Brussels, Belgium.
[2] Service Opera-Photonique, Université libre de Bruxelles, Brussels, Belgium.
[3] Pig For Life SA, Marche-en-Famenne, Belgium.
[4] Synergia Medical SA, Mont-Saint-Guibert, Belgium.
[5] Institute of Neurosciences (IoNS), Université Catholique de Louvain, Brussels, Belgium –Department of Neurology, Cliniques Universitaires Saint Luc, Brussels, Belgium.

Corresponding authors e-mail: louis.vande.perre@ulb.be

Abstract

Background: Infrared neural stimulation (INS) uses short optical pulses to activate nerves. While electrical stimulation (ES) activates large-diameter fibers first, light may preferentially activate small-diameter fibers first, which could be valuable for many clinical applications.

New Method: This study used a compact diode laser of 1470 nm to perform INS. Conduction velocity (CV) measurements were performed to assess differences in fiber type activation between INS and ES in the rat sciatic nerve and the goat vagus nerve. The rat sciatic nerve was chosen as a standard model because of its well-characterized physiology and extensive use in studies of INS mechanisms. The goat vagus nerve was chosen because of its expected high proportion of small-diameter fibers and its larger size, which allows sufficient separation between recording units to optimize CNAP measurements.

Results: The results showed that in the rat sciatic nerve, ES-excited fibers had significantly higher CVs (9.81 ± 3.18 m/s) than INS-excited fibers (8.10 ± 2.82 m/s). In the goat vagus nerve, ES produced a mean CV of 6.47 ± 1.25 m/s, but INS did not produce clearly distinguishable compound nerve action potential, highlighting the challenges of applying INS to larger nerves.

Comparison to Existing Methods: To the best of our knowledge, CV is, for the first time, measured to identify the type of nerve fiber excited by INS.

Conclusion: These results suggest that INS may preferentially activate smaller diameter fibers, providing insight for potential neuromodulation applications.

Keywords: infrared neural stimulation, *ex vivo* rat sciatic nerve, *ex vivo* goat vagus nerve, compound nerve action potential, conduction velocity

1. Introduction

Neurostimulation modulates the nervous system's activity to treat various pathologies, such as deafness, chronic pain, neurodegenerative diseases, and epilepsy (Krames et al., 2009; Vonck et al., 2012). Among the various neural activation techniques, electrical stimulation (ES) has historically been and remains the most common method. However, electrical neuromodulation suffers from various shortcomings. For instance, stimulation artifacts pollute the electrophysiological nerve recordings (Mcgill et al., 1982), the stimulation lacks spatial precision due to electric current spread in the tissues (Liang and Lusted, 1999), and the neurostimulators have a limited compatibility with Magnetic Resonance Imaging (MRI) (Manker and Shellock, 2018). Using near-infrared light to stimulate nerves avoids the stimulation artifact in electrical recording (Wells et al., 2007b), achieves spatial selectivity due to high light absorption in tissue (Izzo et al., 2006; Richter et al., 2011; Sato et al.,

2024; Tian et al., 2024; Wells et al., 2008). It removes the need for metal leads, allowing its compatibility with MRI (Doguet et al., 2024).

Infrared neural stimulation (INS) is the activation of nerve fibers by a transient infrared light exposition. Compared to optogenetic techniques, this method does not require any prior genetic modification of the targeted tissue (Richardson et al., 2020). In the last decade, theoretical developments and *in vitro* experiments have provided a better insight into the mechanism of INS. However, its precise mode of action is not yet fully understood (Beier et al., 2014; Liu et al., 2021; Plaksin et al., 2018). At the same time, *in vivo* experiments have proven the feasibility of this nerve stimulation technique (Cayce et al., 2015; Goyal et al., 2012; Wells et al., 2007a; Yetis et al., 2021).

The order in which the nerve fibers are recruited may also differ between INS and ES. Under physiological conditions, the smaller motor nerve fibers are recruited first (Henneman, 1957; Henneman and Mendell, 1981). In contrast, larger fibers have a lower ES threshold and thus respond first to (even weak) electrical stimuli (Rattay, 1989). Moreover, while ES has been shown to excite mainly the axons of neurons (Ranck, 1975), INS has already been proven to activate neuron soma during *in vitro* experiments (Brown et al., 2013). However, the order in which the nerve fibers are optically recruited is still unknown. An axonal model developed by Fribance et al., based on the widely accepted thermal mechanism, showed that a lower threshold temperature was required to activate small-diameter nerve fibers (Fribance et al., 2016). Based on the cable equation and assuming that the INS mechanism is related to the effect of the temperature gradient on the axonal membrane, Lothet et al. similarly demonstrated that small axons would reach their activation threshold temperature earlier than large axon fibers (Lothet et al., 2017). They further confirmed this prediction by selectively inhibiting the small-diameter fibers of a shrew vagus nerve with infrared light while activating the large-diameter fibers with ES. More recently, Cury et al. reported on late components of the compound nerve action potential (CNAP) evoked by INS, suggesting the activation of small-diameter axons (Cury et al., 2021). Yetis et al. observed a decrease in heart rate and arterial blood pressure during ES of rat vagus nerves, whereas INS only induced a decrease in arterial blood pressure (Yetis et al., 2021). To explain this difference between ES and INS effects, the authors suggested that INS targets small-diameter unmyelinated fibers in the aortic depressor nerve while not exciting the axons that affect heart rate. Overall, these studies point toward INS recruiting small-diameter nerve fibers first, whereas ES does the opposite. However, these data remain hypothetical (e.g., model-based) or preliminary (i.e., on a single trial, as in (Cury et al., 2021)) and need to be confirmed.

The ability to target specific neuronal populations is potentially of significant interest for many neuromodulation therapies. For example, vagus nerve stimulation (VNS) has been implicated in treating various disorders, including epilepsy, depression, obesity, and inflammatory gut disease (Bonaz et al., 2013; McAllen et al., 2018). The applications are diverse, reflecting the range of nerve fiber diameters and functions covered by the vagus nerve (Bonaz et al., 2013). Depending on the desired effect, a specific population of neurons should be targeted to increase treatment efficiency. Unfortunately, common electrical neurostimulators are unable to activate small-diameter axons preferentially (Yuan and Silberstein, 2015). Efforts are underway to develop selective electrical stimulation (Blanz et al., 2023; Musselman et al., 2023) using a patient-specific approach. If INS is shown to activate small-diameter axons intrinsically (i.e., not requiring patient-specific tuning), it would greatly interest many clinical applications.

To better investigate the type of nerve fibers stimulated by INS, we decided to take an experimental approach. Among the techniques used to identify the main type of fibers activated in a nerve, whole nerve conduction velocity (CV) measurements are commonly used (Gasser, 1941; Parker et al., 2018). An experimental setup was developed to record CNAPs at two different locations along the nerve. The rat sciatic nerve was chosen as the first animal model, due to their well-characterized physiology and the availability of background data to validate our experimental setup. In addition, rat sciatic nerves are a common model for understanding INS mechanisms and the effects of stimulus parameters (Coventry et al., 2020; Throckmorton et al., 2021; Wells et al., 2007a). Our interest in small fiber stimulation then required that we also study the cervical vagus nerve, where small-diameter fibers are expected to be abundant in mammals such as rats, pigs, sheep, and humans (Delorme et al., 1997; Pelot et al., 2020; Stakenborg et al., 2020). These features make the vagus nerve an ideal candidate for exploring the potential of INS to target small-diameter fibers selectively. We turned to the goat vagus nerve because it offers a greater length than the rat vagus nerve (~11 mm from (Pelot et al., 2020)), which facilitates hardware design for electrophysiological recording. Moreover, comparing results in two types of animals is also of particular interest, as translating findings from small rodents to larger mammals remains challenging (Rozman and Ribarič, 2019). In this work, CV was first measured in the *ex vivo* rat sciatic nerve using both INS and ES. In the *ex vivo* goat vagus nerve, CV was assessed with ES and histological analysis of tissue thickness was performed to interpret better the mixed results obtained with INS in this larger nerve sample. Finally, the study discusses the CV measured in the rat sciatic nerve with INS compared to ES and highlights the challenges faced in the goat vagus nerve.

Figure 1: Schematic of the experimental setup with two groups of recording electrodes to measure the conduction velocity. Left: rat sciatic nerve. The distal end of the rat sciatic nerve is divided into three smaller branches: sural (a), tibial (b), and peroneal (c). Right: goat vagus nerve

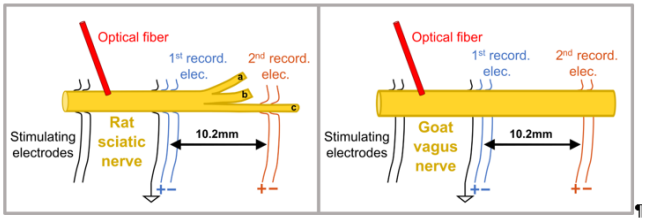

2. Method

Figure 1 shows the experimental setup developed to record CNAPs in an excised rat sciatic or goat vagus nerve. The setup is composed of an acquisition chain to record the electrophysiological activity of the nerve at two different locations, an electrical stimulator and an optical stimulator. The experimental setup is detailed in (Cury et al., 2021; Vande Perre et al., 2022).

2.1 Surgical procedures

The experiments were conducted on rat sciatic nerves and goat cervical vagus nerves.

The experiments on rats were conducted at the Institute of Neuroscience (IoNs), Université Catholique de Louvain (UCLouvain). The left sciatic nerve of seventeen male Wistar rats (3-5 months, 350-420g) were used. The animal care facility is accredited by the Animal Care Service of the Federal Public Department (LA number: 2230419). This work was performed in accordance with a protocol approved by the Ethics Committee for Animal Experimentation at UCLouvain (2022/UCL/MD/011), in compliance with the European Convention ETS 123.

The surgical procedure is briefly described below (for further details, see (Cury et al., 2021)). The animal is anesthetized with an initial intraperitoneal injection of ketamine (60 mg/kg body weight) and xylazine (7 mg/kg body weight). Anesthesia is maintained until the sacrifice by additional bolus injections of ketamine (60 mg/kg body weight) whenever a withdrawal response to noxious paw stimulation is observed, which is checked every 10 minutes. To expose the sciatic nerve, the superficial layer of the thigh muscle is dissected between the gluteus superficialis and biceps femoris muscles. A sciatic nerve length of 30 mm is often achieved, although this depends on where the nerve divides into the peroneal, tibial, and sural branches.

The experiments on five Saanen goats were conducted in cooperation with Pig For Life (PFL) and CER Groupe in Marche-en-Famenne, Belgium, in compliance with Belgian ethics regulations (LA number: 1800104). Ten goat vagus cervical nerves were harvested for *ex vivo* experiments.

The animal is first anesthetized with diazepam (0.3 mg/kg) and then euthanized with pentobarbital (1 ml/kg). All solutions are injected intravenously through a catheter placed in the cephalic vein. Death is confirmed by the absence of cardiac and respiratory movements for at least one minute in compliance with the respective Belgian regulations. Immediately post-mortem, the animal is placed in lateral decubitus, with the head in extension. A skin incision is made above the jugular vein. Soft tissues are dissected while maintaining our position above the jugular vein to reach the vagus nerve. Tissue adjacent to the nerve is carefully discarded while avoiding damage to the nerve. After placing two clamps, the nerve is sectioned to obtain approximately 40 mm of nerve. The sample is immediately placed in a collection tube (preoxygenated Krebs-Ringer solution). The procedure is repeated on the contralateral side.

2.2 Electrical recording and stimulation

Each recording bipolar channel input consists of a pair of electrodes (cathode and anode) separated by 2.5 mm. The two recording channels have their cathodes separated by 10.2 mm, which is thus the conduction distance. A reference electrode is placed between the recording and the stimulating electrodes in order to minimize the amplitude of the stimulation artifact. The acquisition chain is composed of a preamplifier (gain: 40 dB), an amplifier (gain: 28 dB), an isolation stage (gain: -10 dB), and a filtering stage (High-pass of first-order), with a 10-8000 Hz bandwidth.

The overall resolution of this channel is 0.20 µV with a dynamic range of ±3.46 mV, both referred to the input. The measured root mean square noise is 0.43 µV, also referred to the input. The amplifier output is digitized at 40 kHz sampling rate by a DAQ (USB-6212, National Instrument Corp., USA) and processed offline using MATLAB (MathWorks, Natick, USA). This recording setup has been used in (Cury et al., 2022, 2021; Smets et al., 2022, 2021; Stumpp et al., 2021, 2020).

Regarding ES, the DAQ, also interfaces with the current-controlled stimulator. The stimulator generates biphasic square current pulses (negative phase of maximum 1.5 mA amplitude and 0.2 ms duration followed by an interphase delay of 10 µs, and finally, a recovery phase of identical to the first phase except for an opposite polarity).

The pulsed infrared laser used to stimulate the nerve optically is a NeoV 1470 nm from NeoLaser (Caesara, Israel). It is a compact diode laser that emits trains of light pulses with a peak power of 10W and a variable repetition rate (0.5-20 Hz). The pulse duration is set to 0.4 ms to deliver 4mJ per pulse to the nerve. A multimode fiber (numerical aperture 0.22, core diameter 400 µm, NeoLaser), that gently touches the surface of the nerve, delivers the light to the sample (see Figure 1).

2.3 Ex vivo *experimental protocol*

In both rat and goat nerves, the sample was placed on the electrodes after excision, according to Figure 1. For the rat sciatic nerve, we electrically and optically stimulate the main trunk of the nerve and record in the peroneal branch, as we previously obtained successful results in this configuration (Cury et al., 2022, 2021; Vande Perre et al., 2023). Apart from this, the protocol was identical for the goat vagus nerve and the rat sciatic nerve. The nerve was moistened with oxygenated (3 L/min) Krebs-Ringer solution (Fisher Scientific, Merelbeke, Belgium) every 5 minutes to prevent desiccation. The nerve was maintained at room temperature (19-22°C) throughout the experiment. Starting with a lower sample temperature diminishes the risk of reaching temperatures above 43°C, where thermal damage has been noticed by Wells et al. (Wells et al., 2007a). ES (0.3 mA to 1 mA biphasic pulses) allowed to verify the ability of the *ex vivo* sample to generate a CNAP. This was repeated after each optical stimulation to verify the integrity of the nerve and the absence of functional damage induced by INS.

For the optical stimulation, a pulse train consisting of pulses of 10 W peak power and 0.4 ms duration (4 mJ energy) was delivered to the nerve. Besides, the pulse duration was progressively increased for the goat vagus nerve to reach 20mJ pulse energy. Note that the local heat accumulation is limited to a 2 mm diameter spot around the optical fiber and does not affect the nerve segment where CV is measured (Vande Perre et al., 2023).

2.4 Histological analysis

The recording and stimulation setup has already been validated in the *ex vivo* rat sciatic nerve (Cury et al., 2022, 2021; Vande Perre et al., 2023), and there is literature on rat sciatic nerve experiments with INS (Wells et al., 2007a, 2005). However, experiments with INS in the goat vagus nerve were not found in the literature. To better understand our novel experimental conclusion, histological analysis was performed. At the end of the experiment, the region that had been optically stimulated was marked with India ink. Subsequently, the sample was fixed with 4% paraformaldehyde for 48 hours. Following fixation, the sample was preserved in phosphate-buffered saline (PBS) at 4°C. Ultimately, the sample was sliced with a microtome, and Masson's trichrome staining was performed. This staining procedure resulted in the blue coloration of connective tissues, thereby facilitating the identification of nerve fiber bundles and surrounding tissues. To estimate the thickness of the connective tissue, we considered four stimulation sites around the nerve (top, bottom, left, right). Since the nerve has an ellipse-like shape, the left-right axis was defined as the largest axis crossing the center, and the top-bottom axis was defined perpendicular to it, also crossing the center. We measured the distance between the surface of the nerve (epineurium) and the first nerve fibers on

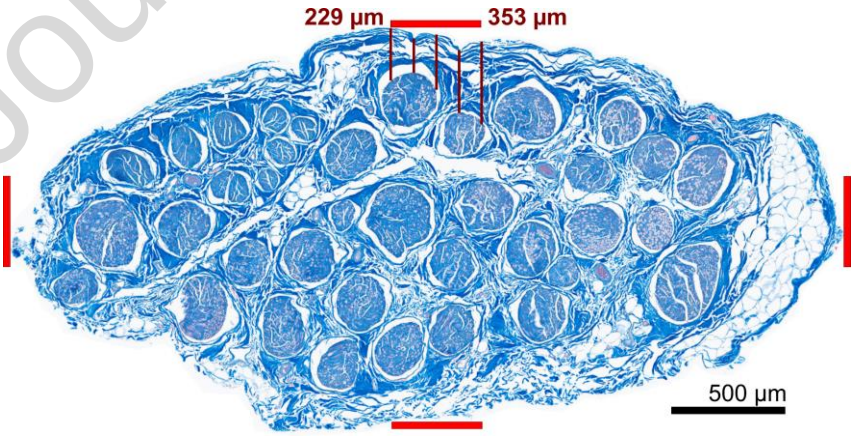

Figure 2: Histological section of the left vagus nerve of goat #4. Masson's trichrome staining shows the connective tissue in blue, surrounding the nerve fiber bundles. Four hypothetical 400 µm wide optical spots (top, bottom, left, right) are shown in red, and the thickness of the surrounding tissue is highlighted for five lateral positions across the excitation beam from the optical spot positioned at the top of the nerve section. The tissue thicknesses measured for the first and last positions are shown as examples.

the path of five beamlines (100 µm between each beam) perpendicular to the optical spot, as shown in Figure 2. This procedure was repeated for the six goat nerve samples we excised from the last three animals sacrificed.

2.5 Compound nerve action potential detection

We implemented a two-step algorithm to validate the presence of CNAPs in the recorded signal from INS trials. First, the signal's root mean squared (RMS) value is computed between 1 ms to 4 ms after the stimulation onset, where a CNAP is expected considering previous experiments (RMS expected CNAP). The RMS value of the signal was also computed from 22 ms to 25 ms after stimulation time (a reference signal at a time when no response is expected). When the RMS expected CNAP value was greater than two times the standard deviation of the reference RMS, it was considered that a CNAP potentially occurred (as previously proposed (Fisher, 1925)). Based on this initial selection of CNAPs, a minimum of 3 epochs of potential CNAPS were averaged to obtain a smoothed version of the CNAP to serve as a template. Second, the cross-correlation between a sliding window of the signal and the template was computed to quantify their similarity. A CNAP was definitely considered present if the cross-correlation of the template where a CNAP is expected (1 ms to 4 ms after the stimulation) was greater than two times the standard deviation of the cross-correlation of the template with the baseline signal.

2.6 Conduction velocity computation

For each experiment, INS and ES trials were used to compute and compare the CV of the excited nerve fibers. The two stimulation methods were run in a sub-minute time interval and under identical conditions (in particular, regarding hydration and nerve temperature). For each modality, the extracellular recording yielded a negative first biphasic potential wave after the stimulus. However, in the case of the rat sciatic nerve, the amplitudes of the responses recorded at the two positions along the length of the nerve differed (See CNAP1 vs CNAP2 in Figure 3). It was expected because the second recording located on the peroneal branch does not see all the fibers stimulated at a more proximal location on the nerve. It results in a lower amplitude of the biphasic potential in the second recording channel. It was not the case for the goat vagus nerve, since no collateral branches left the nerve between the recording points.

An example of the ES and INS CV computations is shown in Figure 3. The CV of the excited nerve fibers was calculated from the time delay between the minimum of the biphasic potential at the first and second pair of electrodes (see, e.g., in Figure 3) (Gu et al., 1996; Stegeman and Weerd, 1982; Žužek et al., 2017).

The CV of ES-evoked CNAPs was calculated from a trace resulting from three averaged epochs. In contrast, INS-evoked CNAPs are more than ten times smaller in amplitude and therefore have a lower SNR. To reliably detect the maximum CNAP, at least ten consecutive INS epochs were averaged before the CV was calculated. Since the slower CVs are less than 1 m/s, and knowing that the distance between the stimulation site and the last electrode is a maximum of 21.6 mm, a time window from 0 to 25 ms after the stimulation time was analyzed to detect possible late components of the CNAP.

The CVs of CNAPs elicited by INS and ES were compared in two ways. First, the CV obtained in the same nerve and *ex vivo* conditions for consecutive trials (INS then ES) were compared to ensure the most homogeneous results for both types of neurostimulation. While ES is often successful, INS does not always induce an identifiable CNAP (see Section 2.5) in both channels, leaving only a few successful INS trials in some experiments. Therefore, we also included a second comparison in which all CVs obtained were compared to get a

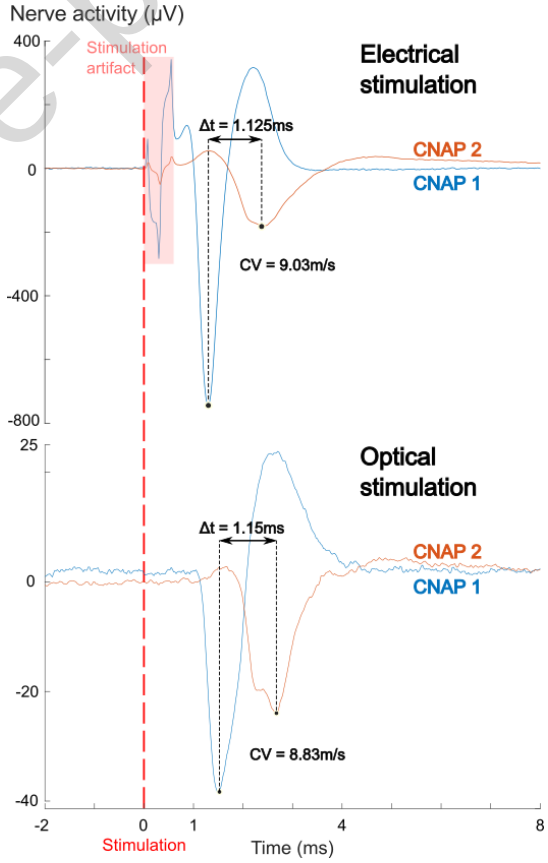

Figure 3: Comparison of conduction velocities of fibers excited by electric current (top) or infrared light (bottom) in rat sciatic nerve #1. The averaged compound nerve action potential (CNAP) recorded by the first and second recording units are shown in blue (CNAP1) and orange (CNAP2), respectively. All Note the difference in scale, which explains the smoother aspect of the top traces.

broader perspective, both for INS and ES, thus increasing the number of samples considered and providing a broader picture of the overall trends.

3. Results

3.1 Rat experiment

Figure 4 shows the CV measured for 22 trials in 10 different rat sciatic nerves, only considering successful and consecutive trials with INS and ES. In most trials (18 out of 22), the CVs of ES-excited fibers were higher than those of INS-excited fibers. The average CV was 9.81±3.18 m/s for ES-excited axons and 8.10±2.82 m/s for INS-excited axons (n=22). A paired sample Wilcoxon signed-rank test was calculated to test whether the difference between ES and INS CVs is a zero median distribution. It confirmed that the ES-excited axon CVs were significantly faster than the INS ones (p-value<0.05).

Considering all successful trials, an average CV of 10.45±4.49 m/s can be computed for ES (n=175), compared to 8.43±3.06 m/s (n=30) in INS. A non-parametric Mann-Whitney test was used (distributions were not normal), showing again that ES-excited axon CVs were significantly faster than INS ones (p-value<0.05).

3.2 Goat experiment

Experiments were performed in five different animals for both left and right vagus nerves. Nine out of ten vagus nerves responded to ES. However, due to the stimulation artifacts or unexpected CNAP shapes, CV could only be calculated in four vagus nerves. Figure 5 shows CNAPs recorded in goat #2 (right vagus nerve) for both recording units in response to ES allowed the CV of excited fibers to be calculated. Among the 15 measurements performed (see Figure 5, right), the average CV was 6.47±1.25 m/s. The amplitude of the measured CNAPs (~25µV in Figure 5) was lower in the goat vagus nerves than in the rat sciatic nerves (~750µV CNAP in Figure 3).

Although performed with a wide range of pulse energies (4 to 20 mJ), none of the trials resulted in a recorded response to INS. Figure 6 shows an unsuccessful INS trial involving the goat #2 (left vagus nerve), despite CNAPs recorded in response to ES before and after the optical stimulation trial. However, upon visual inspection, INS-induced CNAPs of minimal amplitude may still be present. Figure 7 displays a potential response to INS in one trial (right vagus nerve of goat #4), with an amplitude of less than 0.2 µV. The thickness of fat and connective tissue between the nerve surface (where the optical spot is in contact with the tissue) and the nerve fascicle was measured. As shown in Figure 8A, tissue thickness averaged 385 ± 264 µm across 120

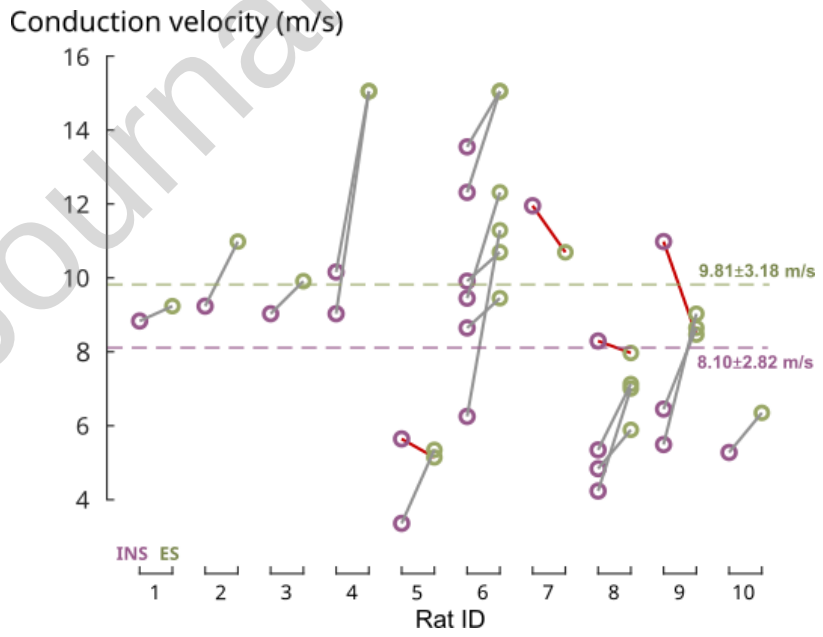

Figure 4: Computed conduction velocities from both electrical stimulation (ES) in green and infrared neural stimulation (INS) in purple. Each INS trial is associated with a line to the ES trial performed consecutively. Red lines highlight cases where CV of the INS trial is higher than the ES' CV. Dashed lines indicate the average CV compute among the ES and INS trials.

measurements from six nerve samples. Special attention was given to the smallest distance between the optical spot and the nearest fiber bundle to better assess the feasibility of nerve fiber stimulation. The average minimum thickness for each hypothetical spot (n=60) was 243 ± 176 µm. For comparison, a typical slice of rat sciatic nerve, a common model used in previous experiments, is shown in Figure 8C, and tissue thickness is estimated to range from a few tenths of µm to 150 µm in the worst case. In addition, the goat vagus nerve has a loose and irregular structure, as shown in Figure 8B, with small-diameter nerve fibers organized into multiple bundles. This architecture, combined with the increased tissue thickness, may explain the difficulty in recording INS-induced CNAPs in the goat vagus nerve compared to the rat sciatic nerve. (Mayrhofer-Schmid et al., 2024)

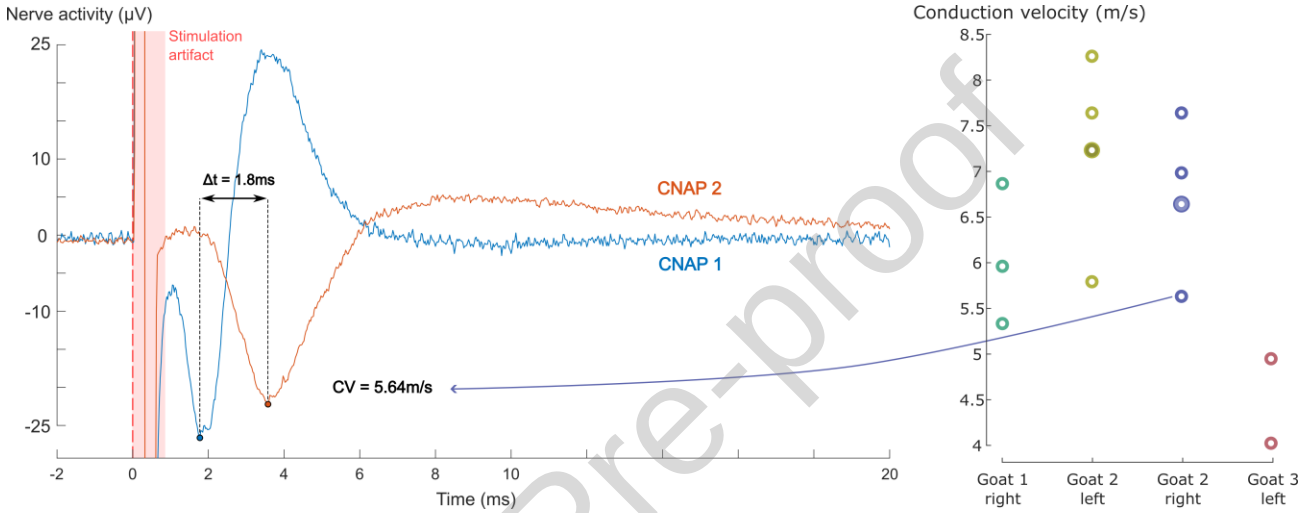

Figure 5: (left) Recording of the compound nerve action potential (CNAP) elicited by electrical stimulation (ES) in the second goat's right vagus nerve. Traces recorded by the first and second recording units are shown in blue and orange, respectively. (right) Summary of the conduction velocities recorded in 4 different goat vagus nerves.

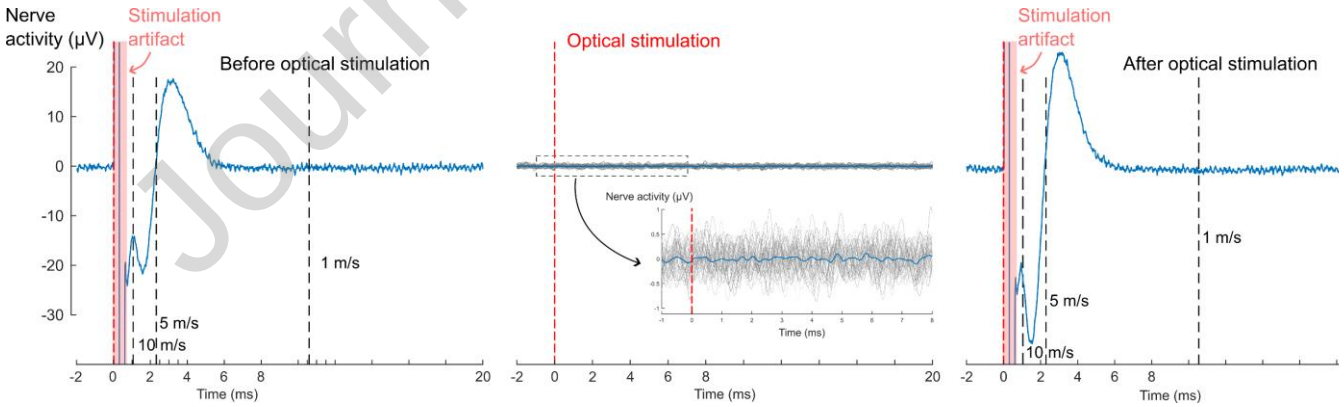

Figure 6: Comparison of successful electrical stimulation before (left) and after (right) the unsuccessful optical stimulation (center) in the left vagus nerve of the second goat. Blue traces are recorded with the first recording unit (after filtering and averaging). Black dashed lines indicate the expected latency of CNAP for different CVs. The magnified graph highlights the lack of recorded response to infrared neural stimulation (INS) despite a pulse energy of 10 mJ. Gray traces represent the 45 epochs averaged to plot the blue line.

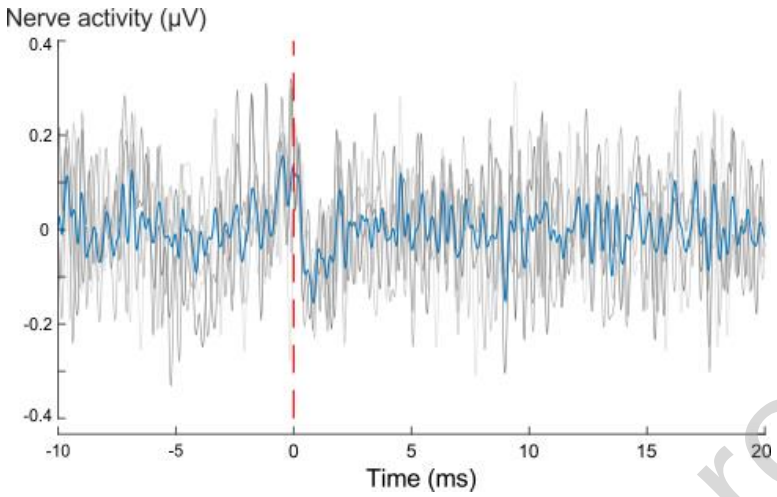

Figure 7: In the fourth goat right vagus nerve, the first trial of optical stimulation with a pulse energy of 4 mJ may have elicited a low-amplitude response to infrared neural stimulation (INS). The blue trace was recorded with the first recording unit (after filtering and averaging). Gray traces represent the 54 epochs averaged to plot the blue line.

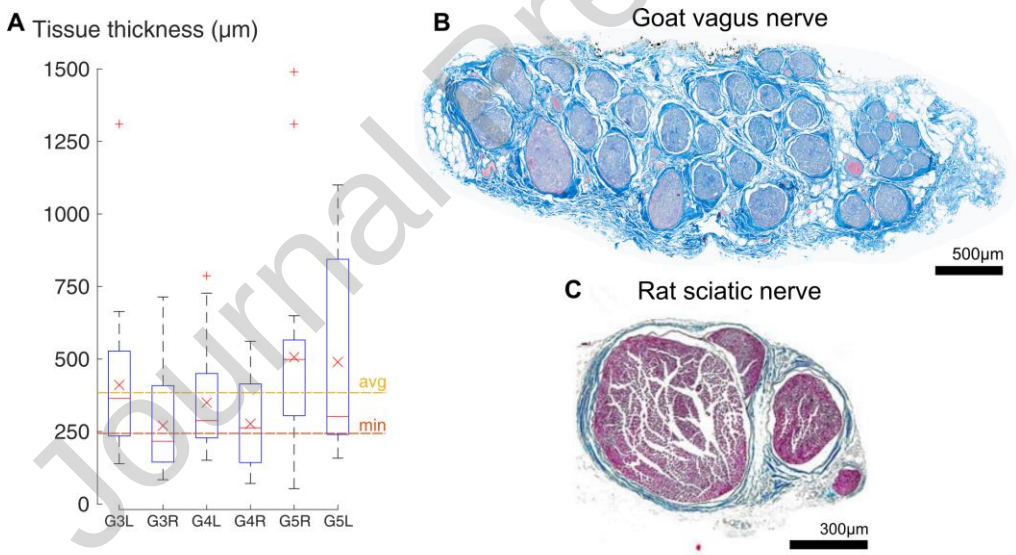

Figure 8: (A) Boxplot of the tissue thickness for the goat vagus nerve #3, #4, and #5, both left (L) and right (R) samples. For each sample, the red cross is the mean value for all tissue thicknesses measured, while the line is the median The yellow dashed line indicates the average of all the tissue thicknesses measured. The orange dashed line indicates the average of the minimum tissue thickness found for each optical spot. (B) Histological section of the right vagus nerve of goat #3. Masson's trichrome staining reveals the connective tissue in blue, surrounding the nerve fiber bundles. (C) For comparison, section of a rat sciatic nerve, stained with Masson's trichrome. Adapted from (Mayrhofer-Schmid et al., 2024), published under CC BY 4.0 license.

4. Discussion

This work investigated the CVs of nerve fibers excited by infrared and electrical stimulation in rats and goats. Whole nerve recording was chosen to record a large population of neurons. The experimental results in rats show that the mean CV of ES-excited fibers was significantly higher than that of INS-excited fibers. To the best of our knowledge, this is the first time that CV measurements of INS-excited axons have been performed and used to investigate the type of fibers activated by optical stimulation. In addition, we extended our investigation to the goat vagus nerve, which contains a higher proportion of smaller diameter fibers compared to the rat sciatic nerve. However, in our experiments, INS only resulted in questionable responses in the goat vagus nerve, underscoring the current challenges in translating this neurostimulation technique to larger nerves.

4.1 Type of fibers excited by electrical and optical stimulation in the rat sciatic nerve

In this work, a mean CV of 9.81±3.18 m/s was obtained in the rat sciatic nerve. It is within the range reported in the literature in *ex vivo* experiments (at room temperature) and compatible with *in vivo* ones (at body temperature). To our knowledge, Žužek et al. were the only ones to record CV in *ex vivo* rat sciatic nerves. They recorded a mean CV of 11.7 m/s on an excised rat sciatic nerve using an ES and a recording setup similar to ours (Žužek et al., 2017). Also, using an *ex vivo* sciatic nerve, but from a mouse, Cargill et al. recorded a mean CV of 10.6 m/s based on the latency of electrically evoked CNAP (Cargill et al., 2008). However, they were unable to record optically evoked CNAP. Back to the rat sciatic nerve but under different conditions (*in vivo* experiment), Huseyinoglu et al. measured a mean CV of 58.90±2.39 m/s (Huseyinoglu et al., 2013). Similarly, Dalkilic et al. measured a CV of 55.7±2.6 m/s, also in the rat sciatic nerve (Dalkilic et al., 2009). A CV of 8±3 m/s was reported from *ex vivo* pig sciatic nerve (Tarotin et al., 2022). Similarly, Ribeiro et al. observed a CV of 16.7 m/s at 20°C in excised porcine ulnar nerve, which increased to 37.7 m/s at 37°C (Ribeiro et al., 2024). The difference between *ex vivo* and *in vivo* experiments can be explained by the difference between the body temperature (37°C) and the temperature at which *ex vivo* experiments were conducted (approximately 20°C) (Dioszeghy and Stålberg, 1992; Ribeiro et al., 2024; Žužek et al., 2017).

To account for this, temperature correction methods are often applied to estimate CV at physiological conditions. The degree of temperature dependence can be quantified by the Q_{10} coefficient, which represents the ratio between the rate of a biological process at two temperatures separated by 10°C (Sterratt, 2014). However, Q_{10} values reported in the literature vary, with alternative estimates of 1.15 (Rutten et al., 1998), 1.44 (Lowitzsch et al., 1977), and 1.51 (De Jesus et al., 1973). This variability underscores the challenges of applying a single correction factor universally. Also, these values are typically derived from human nerves and may not accurately reflect rodent nerve physiology.

Nevertheless, considering a Q_{10} of 1.44, as reported by (Lowitzsch et al., 1977), the corrected CVs for ES and INS in the rat sciatic nerve were estimated to 18 m/s and 15 m/s, respectively. These values align with the CV range reported for A-α/β fibers (11–26 m/s) (Villière and McLachlan, 1996) and are not far from the range reported for A-δ fibers (3–14 m/s). Beyond the identification of precise fiber types, the measured difference of 1.7 m/s (corrected to 3 m/s at 37°C) suggests that ES and INS likely activate different fiber populations. Still, the interpretation of activated fiber types based on CV must remain cautious and other factors, such as nerve fiber myelination, should also be considered (Whitwam, 1976).

Finally, to avoid confusion with stimulus artifacts, we chose to calculate the CV based on the peak of the CNAP rather than its onset, which provides an approximation of the average CV of the excited axons (Žužek et al., 2017). Indeed, the CV of fast (i.e., large-diameter) fibers can be difficult to estimate due to the stimulation artifact. The rat sciatic nerve comprises a heterogeneous population of fibers, with large-diameter fibers contributing disproportionately to the CNAP due to their significant surface area and higher CVs (Birren and Wall, 1956; Castro et al., 2008; Schmalbruch, 1986). While large myelinated fibers dominate the nerve's cross-sectional area, smaller-diameter fibers, such as A-γ/δ and C fibers, are numerically more abundant and carry essential sensory and autonomic functions (Prodanov and Feirabend, 2008). The hook electrodes record a whole nerve rather than individual fibers, providing a good picture of the population of activated nerve fibers, but we may miss activity in small-diameter fibers. Thus, we cannot completely exclude that optical stimulation specifically activates small-diameter fibers, as expected by (Fribance et al., 2016).

4.2 Conduction velocities of goat vagus nerve electrically excited fibers

The ES setup, already validated in several rat experiments (Cury et al., 2022, 2021), was adapted to record the activity of goat vagus nerves. A mean CV of 6.47±1.25 m/s was measured in these nerves. To the best of our knowledge, CVs of goat vagus nerves have never been reported. The closest point of comparison found is a study of the infranodose vagus nerve in sheep, with CVs in the range of 6-12 m/s (Delorme et al., 1997), which is in the same range as our results. However, a mean CV of 72±9.24 m/s in the goat sciatic nerve at body temperature is reported in (Steffen et al., 1996). Similar values were found in the sheep sciatic nerve by (Steiss and Argue, 1987). These higher CV measurements than in our experiments can be attributed

to the distinct fiber compositions and functional roles of these nerves. The sciatic nerve is composed of fast-conducting myelinated fibers, allowing rapid transmission of motor and sensory signals to and from the limbs. In contrast, the vagus nerve is composed of an afferent-to-efferent fiber ratio of approximately 4:1, as reported in studies of mammalian vagus nerves (Hoffman and Schnitzlein, 1961; Verlinden et al., 2016). This higher proportion of small-diameter efferent fibers may explain the slower CV recorded (Delorme et al., 1997).

Finally, the CV obtained through ES is influenced by the stimulation amplitude, with higher amplitudes typically recruiting later components of the CNAP (Parker et al., 2018). In our measurements, the absence of later components can likely be attributed to the lower stimulation amplitudes used (0.5 mA for the rat sciatic nerve and 1.5 mA for the goat vagus nerve). However, this does not affect the main objective of using ES, which was to estimate the CV of the fiber population first triggered by electrical stimulation.

4.3 Challenges in translating optical stimulation in the goat vagus nerve

Although our setup has been validated for recording INS-induced CNAPs in rodents, it failed to record satisfactory responses in the goat vagus nerve when INS was applied. Several factors could have contributed to this outcome. First, heating models for INS suggest that the temperature increase induced by light pulses primarily affects the superficial layers of the nerve and decays rapidly with tissue depth. In the rat sciatic nerve, a maximum temperature increase of approximately 7.5°C was observed at a depth of 100 µm and decreased with depth (Alemzadeh-Ansari et al., 2019). In addition, the heat generated by INS was shown to be confined within 300 µm below the optical fiber in cell culture (Liljemalm et al., 2013). This localized effect of INS has been demonstrated before (Tian et al., 2024; Wells et al., 2007b), but to our knowledge has never been compared in nerve samples of different structure and size. In the case of ES, the morphology of the vagus nerve and the organization of nerve fibers into multiple small bundles has been identified as a challenge to achieve homogeneous stimulation and synchronous recording of the vagus nerve (Pelot et al., 2020; Stakenborg et al., 2020). Similarly, Settell et al. reported a greater amount of connective tissue in the vagus nerve of large mammals (dog, pig, human), which may account for the increased stimulation threshold with ES compared to the rodent vagus nerve (Settell et al., 2020). While the electric field generated by a bipolar electrode decays proportionally to ~$1/d^2$, where d is the distance from the electrode (Plonsey and Barr, 1995), the intensity of the optical beam is expected to decay exponentially according to the Beer-Lambert law (Liljemalm et al., 2013). Therefore, we would expect a greater influence of the surrounding tissue thickness in the case of INS than ES. In the present work, we observed that the goat vagus nerve in our experiments had an average connective tissue thickness of 385±264 µm, taking into account multiple sites of optical stimulation around the nerve. In contrast, the rat sciatic nerve, in which we successfully recorded optically induced CNAPs, has a reported epineurium thickness of 133 µm (Islam et al., 2012) or 51±26 µm (Hope et al., 2018), depending on the study. Both values are less than the connective tissue thickness measured in the goat vagus nerve. This important difference in tissue thickness and reduced thermal penetration may explain the challenges in achieving optically induced CNAPs in the goat vagus nerve.

However, Cayce et al. have previously successfully stimulated human dorsal spinal roots (1-2 mm in diameter) with a 2120 nm laser (Cayce et al., 2015). The use of a 2120 nm Ho:YAG laser may have lowered the stimulation threshold compared to a 1470 nm diode laser, as suggested by (Throckmorton et al., 2021). Nevertheless, 1470 nm or similar wavelengths have shown positive results in activating peripheral nerves in several studies (Alemzadeh-Ansari et al., 2019; Ansari and Zakeri, 2019; Cury et al., 2021; Dautrebande et al., 2018, 2016; McCaughey et al., 2010; Throckmorton et al., 2021). In addition, according to (Anderson et al., 2006), the 1470 nm wavelength has a 10- to 100-fold lower absorption coefficient in adipose tissue compared to other INS wavelengths (1870 and 2120 nm), which may limit the absorption of light in surrounding tissues.

Finally, optical stimulation might activate only a small fraction of the neural population, undetected by our nerve electrodes that average activity over a large nerve section. A multi-channel recording with multiple dot electrodes covering the nerve periphery might be a solution (Bakkum et al., 2013; Ortiz-Catalan et al., 2013; Rozman and Ribarič, 2019). One might be tempted to increase the stimulation intensity to reach the stimulation threshold deeper in the nerve, but the use of pulse energies higher than a few mJ increases the probability of damage (Brown et al., 2020). In addition, the composition of the vagus nerve, which has a higher proportion of smaller diameter fibers, presents unique challenges that differ from those encountered with the predominantly larger motor neurons of the sciatic nerve (Noller et al., 2019). Although drawing definitive conclusions from exploratory experiments on the goat vagus nerve remains challenging, it does highlight the need for refined methods to enhance the efficacy and accuracy of INS in larger and more complex nerve structures.

4.4 Limitations

Our study faces several limitations that need to be acknowledged. First, the *ex vivo* nature of our experiments, while advantageous for recording single nerve action potentials in a controlled environment, presents challenges related to the

degradation of the nerve sample over time. In this regard, experiments were limited to ~2h to ensure nerve viability. In addition, conducting these experiments at ambient temperature significantly affects CV measurements and complicates direct comparisons with physiological data typically obtained at body temperature (Rasminsky, 1973; You and Mou, 2017). Furthermore, to our knowledge, a damage threshold has never been identified in *ex vivo* peripheral nerve samples during INS. Throckmorton et al. reported that radiant exposures higher than 3 J/cm² caused damage in the rat sciatic nerve *in vivo* (Throckmorton et al., 2021). Furthermore, (Wells et al., 2005) found a damage threshold of 2 J/cm² also in the *in vivo* rat sciatic nerve. In our experiments, as we used 10 W peak pulse power and 400 µs pulse duration, the estimated radiant exposure is ~3 J/cm². Therefore, the parameters used in our experiment could be at the upper limit of safe stimulation parameters. However, the risk of reaching critical temperatures at which thermal damage can occur (~60°C as reported by (Brown et al., 2020)) may have been reduced by starting with the sample at ambient temperature instead of ~35°C in an *in vivo* experiment. Still, the *ex vivo* environment allows the recording of the electrophysiological activity from a single nerve without any polluting signals from surrounding structures (Rapeaux et al., 2022; Ribeiro et al., 2024).

Second, the orthodromic configuration (proximal stimulation and distal recording, see Figure 1) chosen for the rat sciatic nerve affects the number of fibers stimulated and recorded (Valls-Sole et al., 2016). Indeed, the number of nerve fibers decreases as nerve branches leave the central trunk of the sciatic nerve, resulting in a lower amplitude obtained by the second recording channel (Schmalbruch, 1986). However, attempts in the antidromic configuration have been unsuccessful, possibly because the proximal recording averages out the relatively small number of distally recorded fibers.

Finally, in shorter nerves, late components may be masked by the main CNAP components. A different animal model with a greater distance between the recording units could, therefore, help to separate different CNAP components corresponding to different fiber types.

4.5 Further works

Future research in this area should address the limitations identified in the present study and further investigate the potential of INS in larger mammalian models. In addition, alternative recording techniques, including intrafascicular electrode recording (Larson and Meng, 2020), should be considered.

Future work could focus on the deconvolution of recorded CNAPs to better identify the types of INS-stimulated fibers. Since CNAPs represent the summation of individual action potentials generated by nerve fibers, deconvolution could allow the separation of individual fiber contributions, providing a clearer picture of which fibers are being activated. This approach would address a key limitation of current CNAP analysis, where larger-diameter fibers often dominate the recorded signal due to their stronger contributions to the compound response (Krarup, 2004). Deconvolution has been explored in prior studies, although it remains a challenging computational problem (Dong et al., 2020). Techniques for deconvolving CNAPs have been proposed in human and pig models (Dong et al., 2021). However, differences in nerve fiber composition, such as the presence of myelin or not, make direct application of these methods to rat sciatic nerves complex (Strahl et al., 2016). Furthermore, existing methods are founded on assumptions regarding the distribution of nerve CV and fiber recruitment, a subject that remains difficult to specify for INS due to our current limited understanding of its underlying mechanisms.

In addition to CV measurements, functional information about the effects of INS on the fiber type, including histological analysis, immunohistochemistry, or advanced imaging methods, could provide a clinical perspective. Moreover, by using a double stimulation protocol, first electrical and then optical, during the refractory period of the electrical response, the electrical response, which is believed to represent the largest myelinated fibers, can be removed by simple signal subtraction. By incorporating these alternative approaches, the understanding of the neural mechanisms underlying INS can be pursued, perhaps leading to advance clinical application of INS in neuromodulation therapies.

Acknowledgments

L. Vande Perre acknowledges the support of the *Fonds pour la formation à la Recherche dans l'Industrie et dans l'Agriculture* (FRIA, FNRS, Belgium) and the *Fonds David et Alice Van Buuren*. We are grateful for the help provided by Geoffrey Vanbienne in implementing our hardware setup. We would also like to thank Amandine Collin, Justine Allard and Sophie Bottieau for their advice and for conducting the histological analysis at CMMI-diapath. The CMMI is supported by the European Regional Development Fund and the Walloon Region, Belgium [Wallonia-biomed; grant no. 411132–957270; project "CMMI-ULB"].

Competing interests

J. Delbeke reports being a shareholder of Synergia Medical SA, Belgium.

Data Availability Statement

The data that support the findings of this study are available from the corresponding author upon reasonable request.

References

Alemzadeh-Ansari, M.J., Ansari, M.A., Zakeri, M., Haghjoo, M., 2019. Influence of radiant exposure and repetition rate in infrared neural stimulation with near-infrared lasers. Lasers Med. Sci. 34, 1555–1566. https://doi.org/10.1007/s10103-019-02741-4

Anderson, R.R., Farinelli, W., Laubach, H., Manstein, D., Yaroslavsky, A.N., Gubeli, J., Jordan, K., Neil, G.R., Shinn, M., Chandler, W., Williams, G.P., Benson, S. V., Douglas, D.R., Dylla, H.F., 2006. Selective photothermolysis of lipid-rich tissues: A free electron laser study. Lasers Surg. Med. 38, 913–919. https://doi.org/10.1002/lsm.20393

Ansari, M.A., Zakeri, M., 2019. Blind localization of heating in neural tissues induced by a train of the infrared pulse laser. J. Lasers Med. Sci. 10, 264–267. https://doi.org/10.15171/jlms.2019.43

Bakkum, D.J., Frey, U., Radivojevic, M., Russell, T.L., Müller, J., Fiscella, M., Takahashi, H., Hierlemann, A., 2013. Tracking axonal action potential propagation on a high-density microelectrode array across hundreds of sites. Nat. Commun. 4. https://doi.org/10.1038/ncomms3181

Beier, H.T., Tolstykh, G.P., Musick, J.D., Thomas, R.J., Ibey, B.L., 2014. Plasma membrane nanoporation as a possible mechanism behind infrared excitation of cells. J. Neural Eng. 11. https://doi.org/10.1088/1741-2560/11/6/066006

Birren, J.E., Wall, P.D., 1956. Age changes in conduction velocity, refractory period, number of fibers, connective tissue space and blood vessels in sciatic nerve of rats. J. Comp. Neurol. 104, 1–16. https://doi.org/10.1002/cne.901040102

Blanz, S.L., Musselman, E.D., Settell, M.L., Knudsen, B.E., Nicolai, E.N., Trevathan, J.K., Verner, R.S., Begnaud, J., Skubal, A.C., Suminski, A.J., Williams, J.C., Shoffstall, A.J., Grill, W.M., Pelot, N.A., Ludwig, K.A., 2023. Spatially selective stimulation of the pig vagus nerve to modulate target effect versus side effect. J. Neural Eng. 20. https://doi.org/10.1088/1741-2552/acb3fd

Bonaz, B., Picq, C., Sinniger, V., Mayol, J.F., Clarençon, D., 2013. Vagus nerve stimulation: From epilepsy to the cholinergic anti-inflammatory pathway. Neurogastroenterol. Motil. 25, 208–221. https://doi.org/10.1111/nmo.12076

Brown, W.G.A., Needham, K., Begeng, J.M., Thompson, A.C., Nayagam, B.A., Kameneva, T., Stoddart, P.R., 2020. Thermal damage threshold of neurons during infrared stimulation. Biomed. Opt. Express 11, 2224–2234. https://doi.org/10.1364/BOE.383165

Brown, W.G.A., Needham, K., Nayagam, B.A., Stoddart, P.R., 2013. Whole cell patch clamp for investigating the mechanisms of infrared neural stimulation. J. Vis. Exp. 7–9. https://doi.org/10.3791/50444

Cargill, R., Baumann, T., Jacques, S.L., 2008. Optical stimulation of excised murine sciatic nerve using 1.8-μm wavelength laser. Opt. Interact. with Tissue Cells XIX 6854, 68540I. https://doi.org/10.1117/12.776992

Castro, J., Negredo, P., Avendaño, C., 2008. Fiber composition of the rat sciatic nerve and its modification during regeneration through a sieve electrode. Brain Res. 1190, 65–77. https://doi.org/10.1016/j.brainres.2007.11.028

Cayce, J.M., Wells, J.D., Malphrus, J.D., Kao, C., Thomsen, S., Tulipan, N.B., Konrad, P.E., Jansen, E.D., Mahadevan-Jansen, A., 2015. Infrared neural stimulation of human spinal nerve roots in vivo. Neurophotonics 2, 015007. https://doi.org/10.1117/1.nph.2.1.015007

Coventry, B.S., Sick, J.T., Talavage, T.M., Stantz, K.M., Bartlett, E.L., 2020. Short-wave Infrared Neural Stimulation Drives Graded Sciatic Nerve Activation Across A Continuum of Wavelengths. Proc. Annu. Int. Conf. IEEE Eng. Med. Biol. Soc. EMBS 2020-July, 3581–3585. https://doi.org/10.1109/EMBC44109.2020.9176177

Cury, J., Smets, H., Bouzin, C., Doguet, P., Vanhoestenberghe, A., Delbeke, J., El Tahry, R., Nonclercq, A., Gorza, S.-P., 2022. Optical Birefringence changes in myelinated and unmyelinated nerves: a comparative study. J. Biophotonics 15, e202200028. https://doi.org/10.1002/jbio.202200028

Cury, J., Vande Perre, L., Smets, H., Stumpp, L., Vespa, S., Vanhoestenberghe, A., Doguet, P., Delbeke, J., El Tahry, R., Gorza, S.-P., Nonclercq, A., 2021. Infrared neurostimulation in ex-vivo rat sciatic nerve using 1470 nm wavelength. J. Neural Eng. 18, 056018. https://doi.org/10.1088/1741-2552/abf28f

Dalkilic, N., Tuncer, S., Bariskaner, H., Kiziltan, E., 2009. The effect of tramadol on the rat sciatic nerve conduction: A numerical analysis and conduction velocity distribution study. Yakugaku Zasshi 129, 485–493. https://doi.org/10.1248/yakushi.129.485

Dautrebande, M., Doguet, P., Gorza, S.-P., Delbeke, J., Botquin, Y., Nonclercq, A., 2016. In vivo Photonic Stimulation of Sciatic Nerve with a 1470 nm Laser. Eur. J. Transl. Myol. 26, 244–248. https://doi.org/10.4081/ejtm.2016.6028

Dautrebande, M., Doguet, P., Gorza, S.-P., Delbeke, J., Nonclercq, A., 2018. Peripheral nerve recruitment curve using near-infrared stimulation, in: Optogenetics and Optical Manipulation 2018. p. 104820V. https://doi.org/10.1117/12.2288398

De Jesus, P. V., Hausmanowa-Petrusewicz, I., Barchi, R.L., 1973. The effect of cold on nerve conduction of human slow and fast nerve fibers. Neurology 23, 1182–1189. https://doi.org/10.1212/wnl.23.11.1182

Delorme, P., Rousseau, A., Bernard, J., Leek, B.F., Rousseau, J.P., 1997. Ultrastructural changes in the nerve fiber population of anastomosed vagal and spinal accessory nerves in the sheep. Anat. Rec. 248, 129–136. https://doi.org/10.1002/(SICI)1097-0185(199705)248:1<129::AID-AR15>3.0.CO;2-R

Dioszeghy, P., Stålberg, E., 1992. Changes in motor and sensory nerve conduction parameters with temperature in normal and diseased nerve. Electroencephalogr. Clin. Neurophysiol. Evoked Potentials 85, 229–235. https://doi.org/10.1016/0168-5597(92)90110-W

Doguet, P., Garnier, J., Nieuwenhuys, A., Godfraind, C., Botquin, Y., Lemaire, A., Justice, J., Nonclercq, A., El Tahry, R., Corbett, B., Delbeke, J., 2024. An optoelectronic implantable neurostimulation platform allowing full MRI safety and optical sensing and communication. Sci. Rep. 14, 1–19. https://doi.org/10.1038/s41598-024-61330-w

Dong, Y., Briaire, J.J., Biesheuvel, J.D., Stronks, H.C., Frijns, J.H.M., 2020. Unravelling the temporal properties of human eCAPs through an iterative deconvolution model. Hear. Res. 395, 108037. https://doi.org/10.1016/j.heares.2020.108037

Dong, Y., Stronks, H.C., Briaire, J.J., Frijns, J.H.M., 2021. An iterative deconvolution model to extract the temporal firing properties of the auditory nerve fibers in human eCAPs. MethodsX 8, 101240. https://doi.org/10.1016/j.mex.2021.101240
Fisher, R.A., 1925. Statistical Methods for Research Workers. Oliver and Boyd, Edinburgh, Scotland.
Fribance, S., Wang, J., Roppolo, J.R., de Groat, W.C., Tai, C., 2016. Axonal model for temperature stimulation. J. Comput. Neurosci. 41, 185–192. https://doi.org/10.1007/s10827-016-0612-x
Gasser, H. s., 1941. Classification of Nerve Fibers. Ohio J. Sci. 41, 145–159. https://doi.org/10.5005/jp/books/11696_49
Goyal, V., Rajguru, S.M., Matic, A.I., Stock, S.R., Richter, C.P., 2012. Acute Damage Threshold for Infrared Neural Stimulation of the Cochlea: Functional and Histological Evaluation. Anat. Rec. 295, 1987–1999. https://doi.org/10.1002/ar.22583
Gu, D., Gander, R.E., Crichlow, E.C., 1996. Determination of nerve conduction velocity distribution from sampled compound action potential signals. IEEE Trans. Biomed. Eng. 43, 829–838. https://doi.org/10.1109/10.508545
Henneman, E., 1957. Relation between Size of Neurons and Their Susceptilbility to Discharge. Science (80-.). 126, 1345–1347. https://doi.org/10.1126/science.126.3287.1345
Henneman, E., Mendell, L.M., 1981. Functional Organization of Motoneuron Pool and its Inputs. Compr. Physiol. 423–507. https://doi.org/10.1002/cphy.cp010211
Hoffman, H.H., Schnitzlein, H.N., 1961. The numbers of nerve fibers in the vagus nerve of man. Anat. Rec. 139, 429–435. https://doi.org/10.1002/ar.1091390312
Hope, J., Braeuer, B., Amirapu, S., Vanholsbeeck, F., McDaid, A., 2018. Extracting morphometric information from rat sciatic nerve using optical coherence tomography. J. Biomed. Opt. 23, 1. https://doi.org/10.1117/1.jbo.23.11.116001
Huseyinoglu, N., Ozaydin, I., Huseyinoglu, U., Yayla, S., Aksoy, O., 2013. Minimally Invasive Motor Nerve Conduction Study of the Rat Sciatic and Tail Nerves. Kafkas Univ. Vet. Fak. Derg. 19, 943–948. https://doi.org/10.9775/kvfd.2013.9065
Islam, M.S., Oliveira, M.C., Wang, Y., Park, B.H., Henry, F.P., Randolph, M.A., de Boer, J.F., 2012. Extracting structural features of rat sciatic nerve using polarization-sensitive spectral domain optical coherence tomography. J. Biomed. Opt. 17, 1. https://doi.org/10.1117/1.jbo.17.5.056012
Izzo, A.D., Richter, C.P., Jansen, E.D., Walsh, J.T., 2006. Laser stimulation of the auditory nerve. Lasers Surg. Med. 38, 745–753. https://doi.org/10.1002/lsm.20358
Krames, E.S., Hunter Peckham, P., Rezai, A.R., Aboelsaad, F., 2009. What Is Neuromodulation?, Volume 1. ed, Neuromodulation. Elsevier Ltd. https://doi.org/10.1016/B978-0-12-374248-3.00002-1
Krarup, C., 2004. Compound sensory action potential in normal and pathological human nerves. Muscle and Nerve 29, 465–483. https://doi.org/10.1002/mus.10524
Larson, C.E., Meng, E., 2020. A review for the peripheral nerve interface designer. J. Neurosci. Methods 332, 108523. https://doi.org/10.1016/j.jneumeth.2019.108523
Liang, D.H., Lusted, H.S., 1999. The nerve-electrode interface of the cochlear implant: Current spread. IEEE Trans. Biomed. Eng. 46, 35–43. https://doi.org/10.1109/10.736751
Liljemalm, R., Nyberg, T., Von Holst, H., 2013. Heating during infrared neural stimulation. Lasers Surg. Med. 45, 469–481. https://doi.org/10.1002/lsm.22158
Liu, X., Qiao, Z., Chai, Y., Zhu, Z., Wu, K., Ji, W., Li, D., Xiao, Y., Mao, L., Chang, C., Wen, Q., Song, B., Shu, Y., 2021. Nonthermal and reversible control of neuronal signaling and behavior by midinfrared stimulation. Proc. Natl. Acad. Sci. U. S. A. 118. https://doi.org/10.1073/pnas.2015685118
Lothet, E.H., Shaw, K.M., Lu, H., Zhuo, J., Wang, Y.T., Gu, S., Stolz, D.B., Jansen, E.D., Horn, C.C., Chiel, H.J., Jenkins, M.W., 2017. Selective inhibition of small-diameter axons using infrared light. Sci. Rep. 7, 1–8. https://doi.org/10.1038/s41598-017-03374-9
Lowitzsch, K., Hopf, H.C., Galland, J., 1977. Changes of sensory conduction velocity and refractory periods with decreasing tissue temperature in man. J. Neurol. 216, 181–188. https://doi.org/10.1007/BF00313619
Manker, S.G., Shellock, F.G., 2018. Chapter 24 - MRI Safety and Neuromodulation Systems, in: Krames, E.S., Peckham, P.H., Rezai, A.R. (Eds.), Neuromodulation. Academic Press, pp. 315–337.
Mayrhofer-Schmid, M., Aman, M., Panayi, A.C., Raasveld, F. V., Kneser, U., Eberlin, K.R., Harhaus, L., Böcker, A., 2024. Fibrin Glue Coating Limits Scar Tissue Formation around Peripheral Nerves. Int. J. Mol. Sci. 25. https://doi.org/10.3390/ijms25073687
McAllen, R.M., Shafton, A.D., Bratton, B.O., Trevaks, D., Furness, J.B., 2018. Calibration of thresholds for functional engagement of vagal A, B and C fiber groups in vivo . Bioelectron. Med. 1, 21–27. https://doi.org/10.2217/bem-2017-0001
McCaughey, R.G., Chlebicki, C., Wong, B.J.F., 2010. Novel wavelengths for laser nerve stimulation. Lasers Surg. Med. 42, 69–75. https://doi.org/10.1002/lsm.20856
Mcgill, K.C., Cummins, K.L., Dorfman, L.J., Berlizot, B.B., Luetkemeyer, K., Nishimura, D.G., Widrow, B., 1982. On the Nature and Elimination of Stimulus Artifact in Nerve Signals Evoked and Recorded Using Surface Electrodes. IEEE Trans. Biomed. Eng. BME-29, 129–137. https://doi.org/10.1109/TBME.1982.325019
Musselman, E.D., Pelot, N.A., Grill, W.M., 2023. Validated computational models predict vagus nerve stimulation thresholds in preclinical animals and humans. J. Neural Eng. 20, 036032. https://doi.org/10.1088/1741-2552/acda64
Noller, C.M., Levine, Y.A., Urakov, T.M., Aronson, J.P., Nash, M.S., 2019. Vagus Nerve Stimulation in Rodent Models: An Overview of Technical Considerations. Front. Neurosci. 13, 1–11. https://doi.org/10.3389/fnins.2019.00911
Ortiz-Catalan, M., Marin-Millan, J., Delbeke, J., Håkansson, B., Brånemark, R., 2013. Effect on signal-to-noise ratio of splitting the continuous contacts of cuff electrodes into smaller recording areas. J. Neuroeng. Rehabil. 10. https://doi.org/10.1186/1743-0003-10-22
Parker, J.L., Shariati, N.H., Karantonis, D.M., 2018. Electrically evoked compound action potential recording in peripheral nerves. Bioelectron. Med. 1, 71–83. https://doi.org/10.2217/bem-2017-0005
Pelot, N.A., Goldhagen, G.B., Cariello, J.E., Musselman, E.D., Clissold, K.A., Ezzell, J.A., Grill, W.M., 2020. Quantified Morphology of the Cervical and Subdiaphragmatic Vagus Nerves of Human, Pig, and Rat. Front. Neurosci. 14, 1–19.

https://doi.org/10.3389/fnins.2020.601479
Plaksin, M., Shapira, E., Kimmel, E., Shoham, S., 2018. Thermal Transients Excite Neurons through Universal Intramembrane Mechanoelectrical Effects. Phys. Rev. X 8, 11043. https://doi.org/10.1103/PhysRevX.8.011043
Plonsey, R., Barr, R.C., 1995. Electric Field Stimulation of Excitable Tissue. IEEE Trans. Biomed. Eng. 42, 329–336. https://doi.org/10.1109/10.376126
Prodanov, D., Feirabend, H.K.P., 2008. Morphometric Analysis of the Fiber Populations of the Rat Sciatic Nerve, Its Spinal Roots, and Its Major Branches. J. Comp. Neurol. 508, 85–100. https://doi.org/10.1002/cne
Ranck, J.B., 1975. Which elements are excited in electrical stimulation of mammalian central nervous system: A review. Brain Res. 98, 417–440. https://doi.org/10.1016/0006-8993(75)90364-9
Rapeaux, A., Syed, O., Cuttaz, E., Chapman, C.A.R., Green, R.A., Constandinou, T.G., 2022. Preparation of Rat Sciatic Nerve for Ex Vivo Neurophysiology. J. Vis. Exp. 2022. https://doi.org/10.3791/63838
Rasminsky, M., 1973. The Effects of Temperature on Conduction in Demyelinated Single Nerve Fibers. Arch. Neurol. 28, 287–292. https://doi.org/10.1001/archneur.1973.00490230023001
Rattay, F., 1989. Analysis of Models for Extracellular Fiber Stimulation. IEEE Trans. Biomed. Eng. 36, 676–682. https://doi.org/10.1109/10.32099
Ribeiro, M., Andreis, F.R., Jabban, L., Nielsen, T.G.N. d. S., Smirnov, S. V., Lutteroth, C., Proulx, M.J., Rocha, P.R.F., Metcalfe, B., 2024. Ex-vivo systems for neuromodulation: A comparison of ex-vivo and in-vivo large animal nerve electrophysiology. J. Neurosci. Methods 406, 110116. https://doi.org/10.1016/j.jneumeth.2024.110116
Richardson, R.T., Ibbotson, M.R., Thompson, A.C., Wise, A.K., Fallon, J.B., 2020. Optical stimulation of neural tissue. Healthc. Technol. Lett. 7, 58–65. https://doi.org/10.1049/htl.2019.0114
Richter, C.P., Matic, A.I., Wells, J.D., Jansen, E.D., Walsh, J.T., 2011. Neural stimulation with optical radiation. Laser Photonics Rev. 5, 68–80. https://doi.org/10.1002/lpor.200900044
Rozman, J., Ribarič, S., 2019. A setup for selective infrared stimulation of an isolated porcine vagus nerve. Sensors Actuators, A Phys. 292, 97–104. https://doi.org/10.1016/j.sna.2019.04.010
Rutten, G.J.M., Gaasbeek, R.D.A., Franssen, H., 1998. Decrease in nerve temperature: A model for increased temporal dispersion. Electroencephalogr. Clin. Neurophysiol. - Electromyogr. Mot. Control 109, 15–23. https://doi.org/10.1016/S0924-980X(97)00049-0
Sato, H., Sugimoto, F., Furukawa, R., Tateno, T., 2024. Modulatory Effects on Laminar Neural Activity Induced by Near-Infrared Light Stimulation with a Continuous Waveform to the Mouse Inferior Colliculus In Vivo. eNeuro 11. https://doi.org/10.1523/ENEURO.0521-23.2024
Schmalbruch, H., 1986. Fiber composition of the rat sciatic nerve. Anat. Rec. 215, 71–81. https://doi.org/10.1002/ar.1092150111
Settell, M.L., Pelot, N.A., Knudsen, B.E., Dingle, A.M., McConico, A.L., Nicolai, E.N., Trevathan, J.K., Ezzell, J.A., Ross, E.K., Gustafson, K.J., Shoffstall, A.J., Williams, J.C., Zeng, W., Poore, S.O., Populin, L.C., Suminski, A.J., Grill, W.M., Ludwig, K.A., 2020. Functional vagotopy in the cervical vagus nerve of the domestic pig: Implications for the study of vagus nerve stimulation. J. Neural Eng. 17. https://doi.org/10.1088/1741-2552/ab7ad4
Smets, H., Stumpp, L., Chavez, J., Cury, J., Vande Perre, L., Doguet, P., Vanhoestenberghe, A., Delbeke, J., El Tahry, R., Nonclercq, A., 2022. Chronic recording of the vagus nerve to analyze modulations by the light-dark cycle. J. Neural Eng. 19, 046008. https://doi.org/10.1088/1741-2552/ac7c8f
Smets, H., Stumpp, L., Julémont, N., Cury, J., Debelle, A., Innocenti, B., Vespa, S., Haut, B., Doguet, P., Vanhoestenberghe, A., Delbeke, J., Tahry, R. El, Nonclercq, A., 2021. Analysing vagus nerve spontaneous activity using finite element modelling. J. Neural Eng. 18, 56008. https://doi.org/10.1088/1741-2552/abe68f
Stakenborg, N., Gomez-Pinilla, P.J., Verlinden, T.J.M., Wolthuis, A.M., D'Hoore, A., Farré, R., Herijgers, P., Matteoli, G., Boeckxstaens, G.E., 2020. Comparison between the cervical and abdominal vagus nerves in mice, pigs, and humans. Neurogastroenterol. Motil. 32, 1–8. https://doi.org/10.1111/nmo.13889
Steffen, F., Jaggy, A., Gaillard, C., Fatzer, R., Aeschbacher, G., Blum, J., Tontis, A., 1996. Referenzbereiche von elektrodiagnostischen und Laboruntersuchungen bei jungen Walliser Schwarzhalsziegen. Tierarztl Prax 24, 22–8.
Stegeman, D.F., Weerd, J.P. De, 1982. Modelling compound action potentials of peripheral nerves in situ. I. Model description: evidence for a non-linear relation between fibre diameter and velocity. Electroencephalogr. Clin. Neurophysiol. 54, 436–448.
Steiss, J.E., Argue, C.K., 1987. Normal values for radial, peroneal and tibial motor nerve conduction velocities in adult sheep, with comparison to adult dogs. Vet. Res. Commun. 11, 243–252. https://doi.org/10.1007/BF00570922
Sterratt, D.C., 2014. Q10: The Effect of Temperature on Ion Channel Kinetics. Encycl. Comput. Neurosci. https://doi.org/10.1007/978-1-4614-7320-6_236-1
Strahl, S.B., Ramekers, D., Nagelkerke, M.M.B., Schwarz, K.E., Spitzer, P., Klis, S.F.L., Grolman, W., 2016. Assessing the Firing Properties of the Electrically Stimulated Auditory Nerve Using a Convolution Model, in: van Dijk, P., Başkent, D., Gaudrain, E., de Kleine, E., Wagner, A., Lanting, C. (Eds.), Physiology, Psychoacoustics and Cognition in Normal and Impaired Hearing. Springer, pp. 143–153. https://doi.org/10.1007/978-3-319-25474-6
Stumpp, L., Smets, H., Vespa, S., Cury, J., Doguet, P., Delbeke, J., Hermans, E., Sevcencu, C., Nielsen, T.N., Nonclerq, A., Tahry, R. El, 2020. Recording of spontaneous vagus nerve activity during Pentylenetetrazol-induced seizures in rats. J. Neurosci. Methods 343, 108832. https://doi.org/10.1016/j.jneumeth.2020.108832
Stumpp, L., Smets, H., Vespa, S., Cury, J., Doguet, P., Delbeke, J., Nonclercq, A., El Tahry, R., 2021. Vagus Nerve Electroneurogram-Based Detection of Acute Pentylenetetrazol Induced Seizures in Rats. Int. J. Neural Syst. 31. https://doi.org/10.1142/S0129065721500246
Tarotin, I., Mastitskaya, S., Ravagli, E., Perkins, J.D., Holder, D., Aristovich, K., 2022. Overcoming temporal dispersion for measurement of activity-related impedance changes in unmyelinated nerves. J. Neural Eng. 19. https://doi.org/10.1088/1741-2552/ac669a
Throckmorton, G., Cayce, J.M., Ricks, Z., Adams, W.R., Jansen, E.D., Mahadevan-Jansen, A., 2021. Identifying optimal parameters for

infrared neural stimulation in the peripheral nervous system. Neurophotonics 8, 1–18. https://doi.org/10.1117/1.NPh.8.1.015012
Tian, F., Zhang, Y., Schriver, K.E., Hu, J.M., Roe, A.W., 2024. A novel interface for cortical columnar neuromodulation with multipoint infrared neural stimulation. Nat. Commun. 15. https://doi.org/10.1038/s41467-024-50375-0
Valls-Sole, J., Leote, J., Pereira, P., 2016. Antidromic vs orthodromic sensory median nerve conduction studies. Clin. Neurophysiol. Pract. 1, 18–25. https://doi.org/10.1016/j.cnp.2016.02.004
Vande Perre, L., Chávez Cerda, J., Verstraeten, M., Raffoul, R., Delbeke, J., El Tahry, R., Nonclercq, A., Gorza, S.-P., 2023. Heat accumulation during infrared stimulation impacts the response of ex vivo rat sciatic nerve, in: 2023 45th Annual International Conference of the IEEE Engineering in Medicine & Biology Society (EMBC). IEEE, pp. 1–4. https://doi.org/10.1109/EMBC40787.2023.10340444
Vande Perre, L., Cury, J., Chavez, J., Verstraeten, M., Raffoul, R., Doguet, P., Delbeke, J., El Tahry, R., Gorza, S.P., Nonclercq, A., 2022. A Setup for Conduction Velocities and Temperature Gradients Measurements during Infrared Neurostimulation, in: 2022 IEEE Biomedical Circuits and Systems Conference (BioCAS). Taipei, Taiwan, pp. 453–457. https://doi.org/10.1109/BioCAS54905.2022.9948671
Verlinden, T.J.M., Rijkers, K., Hoogland, G., Herrler, A., 2016. Morphology of the human cervical vagus nerve: Implications for vagus nerve stimulation treatment. Acta Neurol. Scand. 133, 173–182. https://doi.org/10.1111/ane.12462
Villière, V., McLachlan, E.M., 1996. Electrophysiological properties of neurons in intact rat dorsal root ganglia classified by conduction velocity and action potential duration. J. Neurophysiol. 76, 1924–1941. https://doi.org/10.1152/jn.1996.76.3.1924
Vonck, K., Herdt, V. de, Sprengers, M., Ben-Menachem, E., 2012. Neurostimulation for epilepsy, 1st ed, Handbook of Clinical Neurology. Elsevier B.V. https://doi.org/10.1016/B978-0-444-52899-5.00040-X
Wells, J., Bendett, M., Webb, J., Richter, C., Izzo, A., Jansen, E.D., Mahadevan-Jansen, A., 2008. Frontiers in optical stimulation of neural tissues: past, present, and future. Opt. Interact. with Tissue Cells XIX 6854, 68540B. https://doi.org/10.1117/12.776988
Wells, J., Kao, C., Jansen, E.D., Konrad, P., Mahadevan-Jansen, A., 2005. Application of infrared light for in vivo neural stimulation. J. Biomed. Opt. 10, 064003. https://doi.org/10.1117/1.2121772
Wells, J., Kao, C., Konrad, P., Milner, T., Kim, J., Mahadevan-Jansen, A., Jansen, E.D., 2007a. Biophysical mechanisms of transient optical stimulation of peripheral nerve. Biophys. J. 93, 2567–2580. https://doi.org/10.1529/biophysj.107.104786
Wells, J., Konrad, P., Kao, C., Jansen, E.D., Mahadevan-Jansen, A., 2007b. Pulsed laser versus electrical energy for peripheral nerve stimulation. J. Neurosci. Methods 163, 326–337. https://doi.org/10.1016/j.jneumeth.2007.03.016
Whitwam, J.G., 1976. Classification of peripheral nerve fibres: An historical perspective. Anaesthesia 31, 494–503. https://doi.org/10.1111/j.1365-2044.1976.tb12354.x
Yetis, O., Guner, O., Akkaya, I., Guneli, E., Bagriyanik, A., Tozburun, S., 2021. Vagus nerve bundle stimulation using 1505-nm laser irradiation in an in-vivo rat model. J. Biophotonics. https://doi.org/10.1002/jbio.202100197
You, M., Mou, Z., 2017. Model study of combined electrical and near-infrared neural stimulation on the bullfrog sciatic nerve. Lasers Med. Sci. 32, 1163–1172. https://doi.org/10.1007/s10103-017-2222-x
Yuan, H., Silberstein, S.D., 2015. Vagus Nerve Stimulation and Headache. Headache 57, 29–33. https://doi.org/10.1111/head.12721
Žužek, M.C., Rozman, J., Pečlin, P., Vrecl, M., Frangež, R., 2017. Analysis of compound action potentials elicited with specific current stimulating pulses in an isolated rat sciatic nerve. Biomed. Tech. 62, 37–48. https://doi.org/10.1515/bmt-2015-0167

Declaration of Interest Statement

J. Delbeke reports being a shareholder of Synergia Medical SA, Belgium. The other authors declare that they have no known competing financial interests or personal relationships that could have appeared to influence the work reported in this paper

HIGHLIGHTS

- First conduction velocity (CV) measurements using Infrared neural stimulation (INS).
- Electrically stimulated fibers had significantly higher CV than INS-excited fibers.
- INS may preferentially activate smaller diameter nerve fibers.
- First recorded CV of electrically stimulated goat vagus nerves.